Cumulated Double Bonds

International Edition: DOI: 10.1002/anie.201501810
German Edition: DOI: 10.1002/ange.201501810

Cumulene Rotaxanes: Stabilization and Study of [9]Cumulenes**

*Michael Franz, Johanna A. Januszewski, Dominik Wendinger, Christian Neiss, Levon D. Movsisyan, Frank Hampel, Harry L. Anderson, Andreas Görling, and Rik R. Tykwinski**

Abstract: *The stabilization of long [n]cumulenes has traditionally been achieved by placing sterically bulky "protecting groups" at the termini, which shield the reactive carbon chain from unwanted reactions. Herein, we present an alternative strategy: stabilization through threading the sp-hybridized carbon chain through a phenanthroline-based macrocycle. The result is stable [9]cumulene rotaxanes that enable the study of properties as a function of length for [n]cumulenes in unprecedented detail, including by quantitative UV/Vis spectroscopy, cyclic voltammetry, and differential scanning calorimetry. The experimental results are supported by DFT calculations.*

With the explosion in studies of graphene, fullerenes, and carbon nanotubes, it might seem that interest in carbon allotropes is a relatively new phenomenon.[1] As in the case of many "hot topics", however, there is ample precedent in the literature that such ideas were spawned earlier, although the headlines may not be quite as enticing as they are nowadays. Such is the case with molecules composed of sp-hybridized carbon atoms, namely polyynes and cumulenes, as models for the allotrope carbyne. The chemistry of polyynes expanded dramatically in the 1950s and continues to the present day.[2–5] The synthesis of cumulenes, on the other hand, appeared in the 1930s[6,7] and also took off in the 1950s.[8–14] In 1964, Fischer summarized the results to that point for the handful of known [7]- and [9]cumulenes, concluding that "None of them could be isolated in pure state owing to their instability".[8,11]

Early synthetic work predicted difficulties when assembling "long" cumulenes, similar to the problems encountered in the synthesis of polyynes.[15] As for polyynes,[2–5] the incorporation of sterically demanding end groups has recently facilitated the synthesis of [7]- and [9]cumulenes (Figure 1),

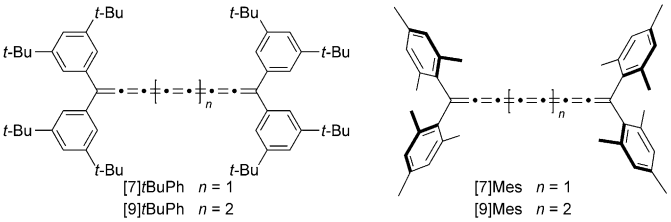

Figure 1. Structures of [7]*t*BuPh, [9]*t*BuPh, [7]Mes, and [9]Mes.

and crystallographic analysis could be done for all but [9]*t*BuPh.[10] [9]Cumulenes are, however, difficult to handle in solution, thus precluding the analysis of many properties. The use of sterically shielding end groups to stabilize cumulenes has seemingly reached a practical limit. An alternative stabilization strategy would be to encapsulate the cumulene core, much like insulation encases a metal wire.[16] This approach has been successful for polyynes[17,18] and other systems[19] through the formation of mechanically interlocked rotaxanes.

In this report, we outline a new method for the kinetic stabilization of [9]cumulenes through the synthesis of rotaxanes. The solution- and solid-state stability of the products makes possible, for the first time, the analysis of [9]cumulenes by quantitative UV/Vis spectroscopy and cyclic voltammetry, as well as differential scanning calorimetry.

The synthesis of cumulene rotaxanes required tetrayne precursors **3a**,**b**, which were assembled by using the phenanthroline macrocycles **1a**[17b] and **1b**,[20] respectively (Scheme 1). The homocoupling reaction of diyne **2a** in the presence of **1a**·Cu gave **3a** in good yield (67%). The use of a smaller macrocycle **1b**·Cu and diyne **2a** also gave the desired rotaxane (**3b**), but in disappointingly low yield (5%). A Cadiot–Chodkiewicz heterocoupling[21] with bromoalkyne **2b** and **2a** in the presence of Cu complex **1a**·Cu was slightly more efficient, giving rotaxane **3a** in 74% yield. The same protocol with complex **1b**·Cu, however, gave only a low yield of the rotaxane **3b** (5%).[22]

The synthesis of [9]cumulene rotaxanes **4a**,**b** was completed through reductive elimination with anhydrous $SnCl_2$ in the presence of HCl (Scheme 2). The reaction solution rapidly turned blue and the formation of **4a** and **4b** was judged

[*] M. Franz, Dr. J. A. Januszewski, D. Wendinger, Dr. F. Hampel, Prof. Dr. R. R. Tykwinski
Department of Chemistry and Pharmacy &
Interdisciplinary Center of Molecular Materials (ICMM)
University of Erlangen-Nuremberg (FAU)
Henkestrasse 42, 91054 Erlangen (Germany)
E-mail: rik.tykwinski@fau.de
Homepage: http://www.chemie.uni-erlangen.de/tykwinski
Dr. C. Neiss, Prof. Dr. A. Görling
Lehrstuhl für Theoretische Chemie &
Interdisciplinary Center of Molecular Materials (ICMM)
University of Erlangen-Nuremberg (Germany)
Dr. L. D. Movsisyan, Prof. Dr. H. L. Anderson
Department of Chemistry, University of Oxford (UK)

[**] Funding is gratefully acknowledged from the University of Erlangen-Nuremberg, the Deutsche Forschungsgemeinschaft (DFG) (SFB 953 "Synthetic Carbon Allotropes" and DFG grant "Rotaxane-Protected Polyynes and Cumulenes"). L.D.M. was supported by an Oxford University Raffy Manoukian Scholarship.

Supporting information for this article is available on the WWW under http://dx.doi.org/10.1002/anie.201501810.

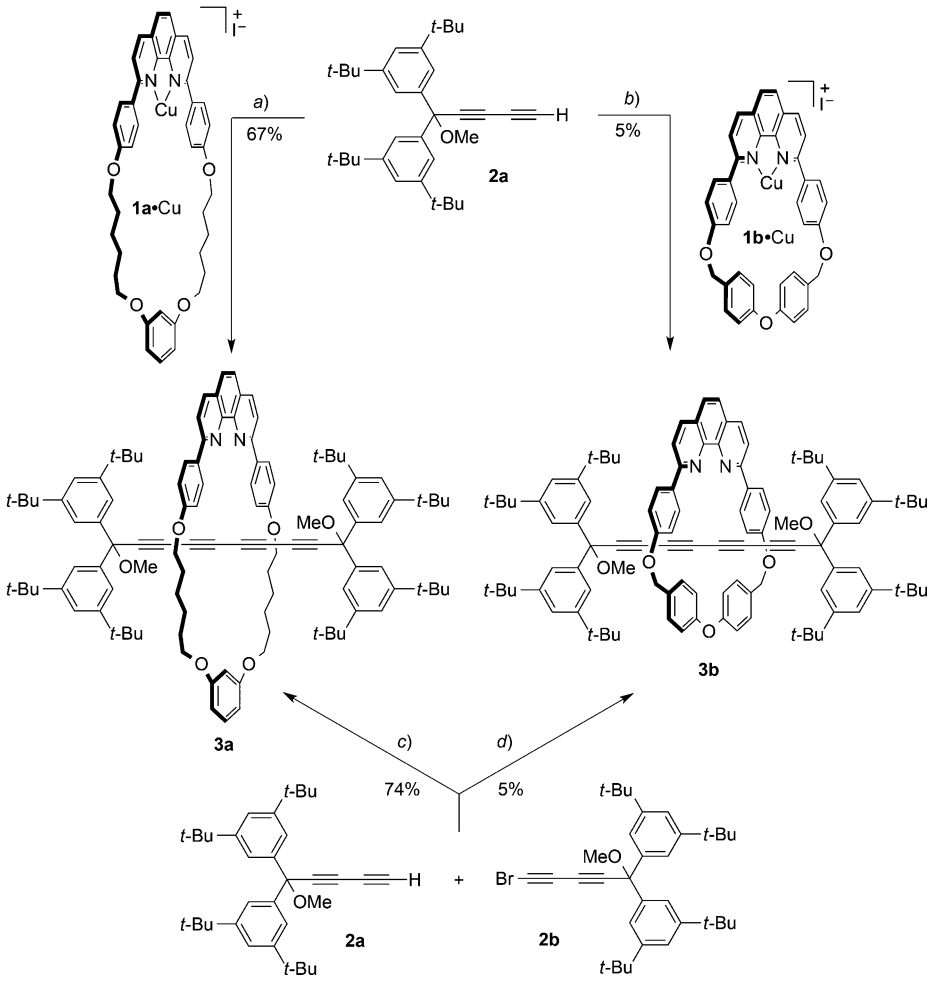

Scheme 1. Synthesis of rotaxanes **3a** and **3b.** Reagents and conditions: a) **1a**·Cu, K_2CO_3, I_2, THF, 60 °C, 4–24 h. b) **1b**·Cu, K_2CO_3, I_2, THF, 60 °C, 45–65 h. c) **1a**·Cu, K_2CO_3, THF, 60 °C, 4 h. d) **1b**·Cu, K_2CO_3, THF, 60 °C, 65 h. THF = tetrahydrofuran.

complete within 1 h. The solutions were neutralized by filtration through basic alumina, and pure **4a** and **4b** were obtained through recrystallization.

Single crystals of **3b** have been analyzed by X-ray crystallography (Figure 2 and Figure S1 in the Supporting Information). The solid-state structure confirms the threading of the axle through macrocycle **1b**. The solid-state structure also offers an explanation for the low yields achieved with **1b**: the steric demands observed for the product are likely reflected in the formation of **3b**, which lowers the yield of the desired rotaxane.

It should be noted in the structure of **3b** that the polyyne chain bends as it threads, with bond angles from 170.9° to 174.2°,[23] and the bending appears to be due to dispersive/van der Waals forces. For example, the electron-deficient polyyne chain is closely embraced by the electron-rich diaryl ether unit; the closest distance between the polyyne and the sp^2-hybridized carbon atoms of the diaryl ether is 3.42 Å, less than twice the van der Waals radius (ca. 1.75 Å).[24] The polyyne also makes close contacts with the electron-rich aryl groups bonded to the phenanthroline unit (shortest distance 3.40 Å), and the closest contact between the C–H groups of these aryl moieties and the polyyne carbon atoms is 2.82 Å, consistent with C–H/π interactions.[25] Finally, C–H/π attractions between the *tert*-butyl groups and the aryl groups of the rotaxane ring also appear to play a role. DFT calculations confirm the influence of dispersive interactions (see the Supporting Information for computational details) since calculations for **3b** that do not take into account van der Waals interactions lead to a linear conformation of the polyyne. Upon the inclusion of dispersion interactions in the calculations, however, the polyyne chain assumes a bent geometry. Calculations for the cumulene rotaxane **4b** predict analogous behavior, i.e., bending of the cumulene chain owing to van der Waals interactions.

The persistence (kinetic stability) of [9]cumulene rotaxanes **4a** and **4b** in solution and as solids raised one of the most interesting questions, since neither [9]*t*BuPh nor [9]Mes are stable. Oxygen-free solutions of rotaxane **4a** and the [9]cumulene [9]*t*BuPh in Et_2O were kept under argon at room temperature and compared. The blue solution of [9]*t*BuPh decolorized within 3 h under exposure to ambient light and overnight if kept in the dark. The analogous solution of **4a** maintained a blue color for about one week under ambient light and for

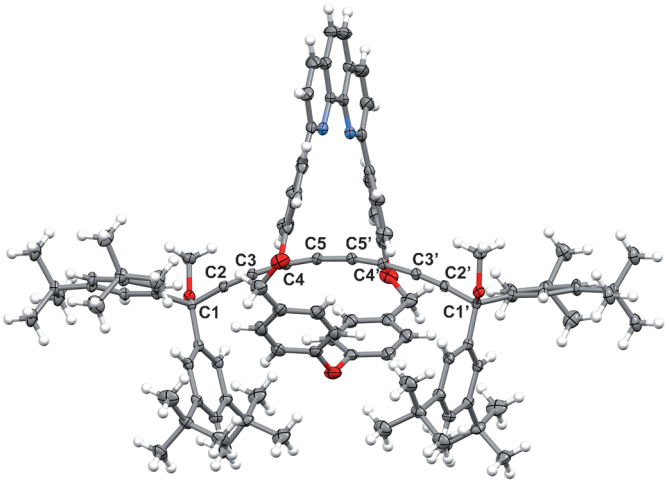

Figure 2. ORTEP of **3b**. Selected bond angles [°]: C2-C3-C4 174.2(2), C3-C4-C5 172.7(2), C4-C5-C5′ 170.89(13).

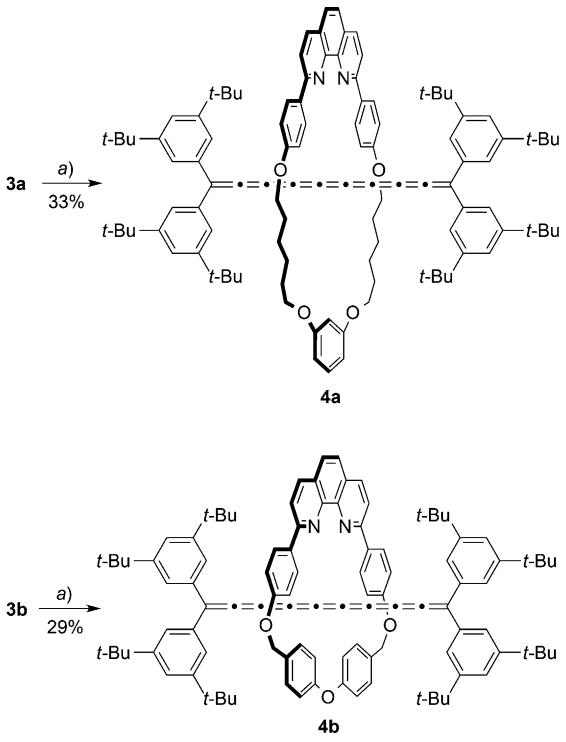

Scheme 2. Synthesis of [9]cumulene rotaxanes **4a** and **4b**. Reagents and conditions: a) $SnCl_2$ (anhydrous), HCl (1 M in Et_2O), Et_2O, Ar, room temperature.

several weeks in the dark. Rotaxanes **4a** and **4b** could be purified by recrystallization from solutions of CH_2Cl_2/MeOH, and both are stable indefinitely in the crystalline form.[26]

With respect to thermal stability, [5]cumulenes typically show melting points of more than 225 °C,[14] while the [7]cumulene [7]*t*BuPh shows a decomposition point of 160–162 °C (in an open capillary tube).[10] Differential scanning calorimetry (DSC) analysis of [7]*t*BuPh showed an exotherm from decomposition, with onset at 187 °C (peak 215 °C). DSC analysis of **4a** showed no melting point but a sharp exotherm from decomposition (onset 170 °C, maxima at 177 °C and 192 °C).[27] The thermal stability of [7]*t*BuPh and **4a** is thus comparable, in spite of the longer conjugated framework of the latter.

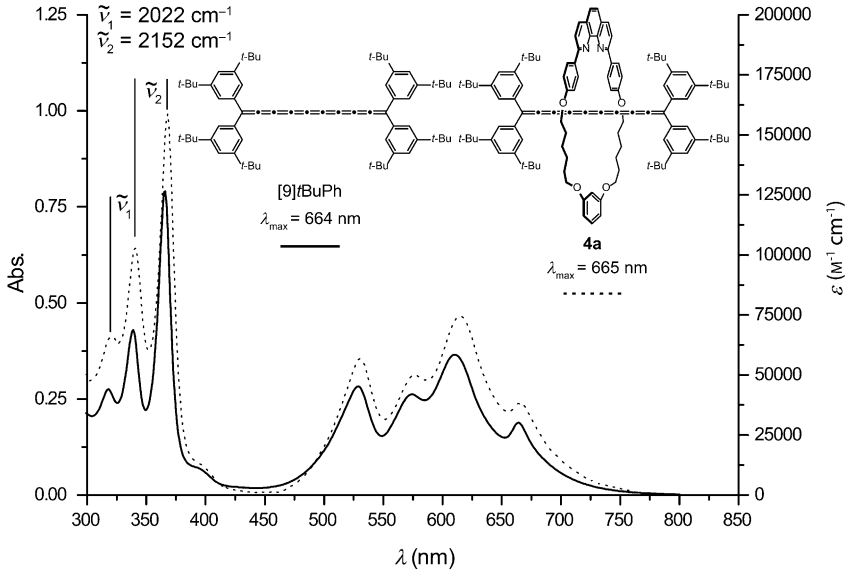

Figure 3. UV/Vis spectra of the naked [9]cumulene [9]*t*BuPh (qualitative) and [9]cumulene rotaxane **4a** (quantitative), measured in Et_2O.

The UV/Vis spectra of [9]*t*BuPh and **4a** show similar absorption features (Figure 3) and the lowest energy absorptions ($\lambda_{max} = 664$ and 665 nm) are essentially the same.[28] According to DFT calculations for [9]*t*BuPh, the λ_{max} absorptions are dominated by the HOMO–LUMO transition. The broadened absorption pattern and vibrational structure observed for the λ_{max} absorptions is clarified by analysis of the frontier molecular orbitals (FMOs), in which involvement of the aryl rings in the composition of the HOMO and LUMO (formed from the out-of-plane π system) is clearly observed (Figure 4). Molar absorptivities for [9]cumulenes have not been previously determined owing to instability of the products. From the spectrum in Figure 3, however, it is clear that **4a** shows significant absorption values, especially in the UV region. A series of three intense signals is observed for **4a** at 319, 341, and 368 nm ($\varepsilon_{368} = 159000$). Interestingly, both the intensity and the vibrational pattern ($\tilde{\nu}_1 = 2022$, $\tilde{\nu}_2 = 2152$ cm^{-1}) of the UV signals for **4a** are analogous to those found for tetraynes.[29] The similarities are explained by DFT calculations performed on [9]*t*BuPh, which showed that these UV absorptions arise mostly from the in-plane π system constructed from the eight sp-hybridized carbon atoms of the cumulene chain. This absorption is dominated by HOMO−1 to LUMO+1 transitions (Figure 4) and the related vibrational levels.

Cyclic voltammetry (CV) offers a detailed analysis of the electronic make-up of the cumulene framework, and the series of stable cumulenes [*n*]*t*BuPh, including [9]cumulene **4a**, gives rather surprising results (Table 1 and Figure S19). First, the redox events for all of the cumulenes are reversible or quasi-reversible, except for the oxidation of **4a**, which is undoubtedly rendered irreversible by the presence of the phenanthroline unit.[30] The reversible behavior is striking[31] given that CV analysis of polyynes shows mostly irreversibly events.[32] Notably, the first oxidation potential varies little as a function of cumulene length, while the first reduction potential decreases from −2.18 V for [3]*t*BuPh to −1.20 V for **4a**. These data suggest that only the LUMO energy is affected by the molecular length. In fact, DFT calculations confirm that the energy of the HOMO is less affected by variation in the chain length than the energy of the LUMO (Table 1). This can be rationalized qualitatively by a simple "particle in a box" model for the cumulene π electrons.[33,34] The energy

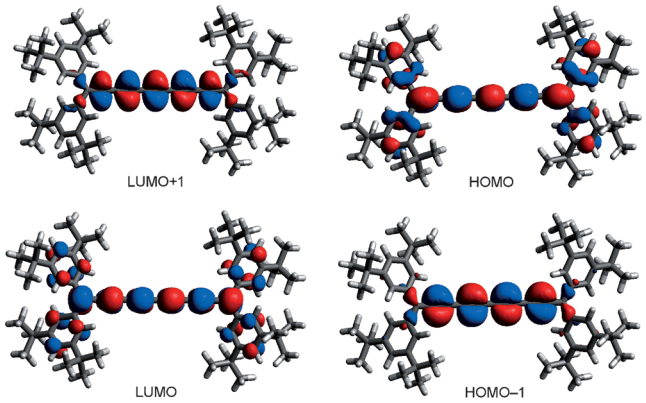

Figure 4. FMOs for [9]*t*BuPh based on DFT calculations. The HOMO and LUMO are formed by the out-of-plane π system with contributions from the terminal aryl rings. The HOMO−1 and LUMO+1 are formed by the in-plane π system and do not extend to the π system of the terminal aryl rings.

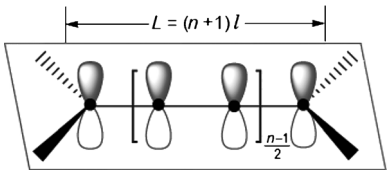

Figure 5. Schematic representation of a [*n*]cumulene. The out-of-plane π system contains $n+1$ π electrons and its length L can be estimated as $L = n \cdot l + l = (n+1)l$, accounting for the fact that the π system extends somewhat over the terminal C atoms ($n = 3, 5, 7, 9, \ldots$).

Table 1: Properties of selected [*n*]cumulenes.

Compound	E_{red1}[a] [V]	E_{red2}[a] [V]	E_{ox1}[a] [V]	E_{ox2}[a] [V]	ε_{HOMO}[b] [eV]	ε_{LUMO}[b] [eV]	$\Delta\varepsilon$[b] [eV]	$E_{g,el}$[c] [eV]	$E_{g,opt}$[d] [eV]	E_g[e] [eV]
[3]*t*BuPh	−2.18		0.49	0.95	−4.99	−2.07	2.92	2.67	2.64 ($CHCl_3$)	2.68
[5]*t*BuPh	−1.72	−2.19	0.43	0.80	−4.89	−2.48	2.41	2.15	2.25 ($CHCl_3$)	2.16
[7]*t*BuPh	−1.37	−1.72	0.42	0.68	−4.87	−2.76	2.11	1.79	1.97 ($CHCl_3$)	1.86
4a	−1.20	−1.56	0.42[f]		−4.86	−2.97	1.89	1.62	1.74 (Et_2O)	1.63

[a] Cyclic voltammetry in CH_2Cl_2 solutions with ferrocene/ferrocenium (Fc/Fc^+) couple as reference (see the Supporting Information). [b] Orbital energies calculated at the B3LYP level (see the Supporting Information); [9]*t*BuPh was considered as a model for **4a**. [c] Electrochemical gaps determined by $E_{g,el} = E_{ox1} - E_{red1}$. [d] Estimated optical gaps from solution-state UV/Vis spectra, based on the intercept of a tangent line applied to the lower edge of the longest wavelength absorption and the *x*-axis. [e] Gaps calculated at the B3LYP level as the difference of twice the total energy of the neutral molecule minus the corresponding energies of the cation and the anion. [f] Irreversible, estimated from peak potential.

levels, ε, of an electron in a one-dimensional box are given by (in atomic units) Equation (1), where m is the quantum

$$\varepsilon = m^2/(8L^2) \quad (1)$$

number of the states (orbitals) and L the box length. In a [*n*]cumulene, the out-of-plane π system forms a box of length $L = (n+1)l$ (Figure 5), in which l is the mean C–C bond length of the cumulene chain. In the [*n*]cumulenes, $n+1$ electrons occupy the out-of-plane π system and the HOMO therefore corresponds to $m = (n+1)/2$. Inserting $L = (n+1)l$ and $m = (n+1)/2$ into Equation (1) for the energy levels leads to the HOMO energy as given in Equation (2).

$$\varepsilon_{HOMO} = 1/(32l^2) \quad (2)$$

The energy of the HOMO is thus independent of the number of double bonds n. The LUMO corresponds to $m = [(n+1)/2]+1$ and the energy ε_{LUMO} thus decreases with increasing length n (Equation (3)).

$$\varepsilon_{LUMO} = 1/(32l^2)(1 + [4/(n+1)] + 4/(n+1)^2) \quad (3)$$

The HOMO–LUMO gaps from the DFT calculations (Table 1, $\Delta\varepsilon$) closely mimic the electrochemically measured gaps for the [*n*]cumulenes ($E_{g,el}$), although they are consistently larger by about 0.3 eV. More accurate gaps (E_g) could be calculated as the difference of twice the total electronic energy of the neutral molecule minus the corresponding energies of the cation and the anion.

To summarize, we have stabilized the typically reactive framework of [9]cumulenes by using two different macrocycles to give cumulene rotaxanes **4a** and **4b**. CV experiments for the series of [*n*]*t*BuPh cumulenes ($n = 3, 5, 7$) and [9]cumulene rotaxane **4a** show that the LUMO energy decreases dramatically with cumulene length (n), while the energy of the HOMO stays approximately constant. The experimental results are in very good agreement with the DFT calculations.

Keywords: carbynes · cumulenes · dispersion forces · electrochemistry · rotaxanes

How to cite: *Angew. Chem. Int. Ed.* **2015**, *54*, 6645–6649
Angew. Chem. **2015**, *127*, 6746–6750

[1] X. Wang, C. D. Liman, N. D. Treat, M. L. Chabinyc, D. G. Cahill, *Phys. Rev. B* **2013**, *88*, 075310; V. Georgakilas, M. Otyepka, A. B. Bourlinos, V. Chandra, N. Kim, K. C. Kemp, P. Hobza, R. Zboril, K. S. Kim, *Chem. Rev.* **2012**, *112*, 6156–6214; H. Omachi, Y. Segawa, K. Itami, *Org. Lett.* **2011**, *13*, 2480–2483.
[2] F. Bohlmann, *Angew. Chem.* **1953**, *65*, 385–389.
[3] R. Eastmond, T. R. Johnson, D. R. M. Walton, *Tetrahedron* **1972**, *28*, 4601–4616.
[4] Q. Zheng, J. C. Bohling, T. B. Peters, A. C. Frisch, F. Hampel, J. A. Gladysz, *Chem. Eur. J.* **2006**, *12*, 6486–6505.
[5] W. A. Chalifoux, R. R. Tykwinski, *Nat. Chem.* **2010**, *2*, 967–971.
[6] R. Kuhn, K. Wallenfels, *Ber. Dtsch. Chem. Ges.* **1938**, *71*, 783–790.
[7] To our knowledge, Kuhn christened this class of compounds "cumulenes" (ref. [6]), while the first cumulene synthesis, albeit

accidental, was reported earlier: K. Brand, *Ber. Dtsch. Chem. Ges.* **1921**, *54*, 1987 – 2006.
[8] H. Fischer, in *The Chemistry of Alkenes* (Ed.: S. Patai), Wiley, New York, **1964**, pp. 1025 – 1159.
[9] B. Bildstein, *Coord. Chem. Rev.* **2000**, *206 – 207*, 369 – 394.
[10] J. A. Januszewski, D. Wendinger, C. D. Methfessel, F. Hampel, R. R. Tykwinski, *Angew. Chem. Int. Ed.* **2013**, *52*, 1817 – 1821; *Angew. Chem.* **2013**, *125*, 1862 – 1867.
[11] A recent summary of extended cumulene syntheses: J. A. Januszewski, R. R. Tykwinski, *Chem. Soc. Rev.* **2014**, *43*, 3184 – 3203.
[12] R. Kuhn, H. Krauch, *Chem. Ber.* **1951**, *84*, 566 – 570.
[13] F. Bohlmann, K. Kieslich, *Abh. Braunschw. Wiss. Ges.* **1957**, *9*, 147 – 166.
[14] Y. Kuwatani, G. Yamamoto, M. Oda, M. Iyoda, *Bull. Chem. Soc. Jpn.* **2005**, *78*, 2188 – 2208.
[15] W. A. Chalifoux, R. R. Tykwinski, *C. R. Chim.* **2009**, *12*, 341 – 358.
[16] J. Stahl, W. Mohr, L. de Quadras, T. B. Peters, J. C. Bohling, J. M. Martín-Alvarez, G. R. Owen, F. Hampel, J. A. Gladysz, *J. Am. Chem. Soc.* **2007**, *129*, 8282 – 8295.
[17] a) S. Schrettl, E. Contal, T. N. Hoheisel, M. Fritzsche, S. Balog, R. Szilluweit, H. Frauenrath, *Chem. Sci.* **2015**, *6*, 564 – 574; b) L. D. Movsisyan, D. V. Kondratuk, M. Franz, A. L. Thompson, R. R. Tykwinski, H. L. Anderson, *Org. Lett.* **2012**, *14*, 3424 – 3426; c) N. Weisbach, Z. Baranová, S. Gauthier, J. H. Reibenspies, J. A. Gladysz, *Chem. Commun.* **2012**, *48*, 7562 – 7564; d) S. Saito, E. Takahashi, K. Nakazono, *Org. Lett.* **2006**, *8*, 5133 – 5136.
[18] J. Berná, J. D. Crowley, S. M. Goldup, K. D. Hanni, A.-L. Lee, D. A. Leigh, *Angew. Chem. Int. Ed.* **2007**, *46*, 5709 – 5713; *Angew. Chem.* **2007**, *119*, 5811 – 5815.
[19] a) E. A. Neal, S. M. Goldup, *Chem. Commun.* **2014**, *50*, 5128 – 5142; b) C. B. Caputo, K. Zhu, V. N. Vukotic, S. J. Loeb, D. W. Stephan, *Angew. Chem. Int. Ed.* **2013**, *52*, 960 – 963; *Angew. Chem.* **2013**, *125*, 994 – 997; c) M. J. Frampton, H. L. Anderson, *Angew. Chem. Int. Ed.* **2007**, *46*, 1028 – 1064; *Angew. Chem.* **2007**, *119*, 1046 – 1083; d) E. Arunkumar, N. Fu, B. D. Smith, *Chem. Eur. J.* **2006**, *12*, 4684 – 4690.
[20] A. M. Blanco-Rodríguez, M. Towrie, J.-P. Collin, S. Záliš, A. Vlček, Jr., *Dalton Trans.* **2009**, 3941 – 3949.
[21] P. Siemsen, R. C. Livingston, F. Diederich, *Angew. Chem. Int. Ed.* **2000**, *39*, 2632 – 2657; *Angew. Chem.* **2000**, *112*, 2740 – 2767.
[22] Synthesis of a tetrayne rotaxane bearing mesityl endgroups was attempted toward forming the [9]Mes rotaxane. Unfortunately, this has not been successful to date, presumably owing to steric hindrance from the mesityl aryl rings.
[23] Bending in polyyne structures: S. Szafert, J. A. Gladysz, *Chem. Rev.* **2006**, *106*, PR1 – PR33.
[24] R. S. Rowland, R. Taylor, *J. Phys. Chem.* **1996**, *100*, 7384 – 7391.
[25] M. Nishio, *Phys. Chem. Chem. Phys.* **2011**, *13*, 13873 – 13900.
[26] "Enhanced" kinetic stabilization has been noted for polyynes in the crystalline state: K. West, L. N. Hayward, A. S. Batsanov, M. R. Bryce, *Eur. J. Org. Chem.* **2008**, 5093 – 5098; S. Eisler, N. Chahal, R. McDonald, R. R. Tykwinski, *Chem. Eur. J.* **2003**, *9*, 2542 – 2550.
[27] DSC scans for [7]*t*BuPh and **4a** are provided as Figures S16 and S17 in the Supporting Information.
[28] The λ_{max} value for **4b** is slightly red-shifted (670 nm; see Figure S18).
[29] R. R. Tykwinski, W. Chalifoux, S. Eisler, A. Lucotti, M. Tommasini, D. Fazzi, M. Del Zoppo, G. Zerbi, *Pure Appl. Chem.* **2010**, *82*, 891 – 904.
[30] J.-B. Raoof, R. Ojani, D. Nematollahi, A. Kiani, *Int. J. Electrochem. Sci.* **2009**, *4*, 810 – 819. See also Ref. [17c].
[31] Enhanced stability of a cyanine dye upon rotaxane formation has been observed: C. M. S. Yau, S. I. Pascu, S. A. Odom, J. E. Warren, E. J. F. Klotz, M. J. Frampton, C. C. Williams, V. Coropceanu, M. K. Kuimova, D. Phillips, S. Barlow, J.-L. Brédas, S. R. Marder, V. Millar, H. L. Anderson, *Chem. Commun.* **2008**, 2897 – 2899.
[32] W. A. Chalifoux, M. J. Ferguson, R. McDonald, F. Melin, L. Echegoyen, R. R. Tykwinski, *J. Phys. Org. Chem.* **2012**, *25*, 69 – 76.
[33] For cumulenes as a "particle in a box", see among others: S. Hino, Y. Okada, K. Iwasaki, M. Kijima, H. Shirakawa, *Chem. Phys. Lett.* **2003**, *372*, 59 – 65.
[34] Treatment of cumulenes by extended Hückel theory: R. Hoffmann, *Tetrahedron* **1966**, *22*, 521 – 538.

Received: February 27, 2015
Published online: April 27, 2015

